Vol. 47, No. 3 (2025) 526-537, DOI: 10.24874/ti.1967.04.25.07

Tribology in Industry

www.tribology.rs

RESEARCH

Enhancement of Diesel Engine Performance and Emission Control Through Thermal Barrier Coating of $Sm_2Zr_2O_7$ and Al_2O_3–13%TiO_2 on the Piston

T. Chandrashekar[a,*], M.M. Nataraja[a], J. Balaji[a], L. Bangarappa[b], K. Sadashiva[a]

[a]*Department of Mechanical Engineering, Dr Ambedkar Institute of Technology, VTU, Belgaum, Karnataka, India.*
[b]*Department of Mechanical Engineering, University of Visvesvaraya College of Engineering, Bengaluru University, India.*

Keywords:

Thermal barrier coating
Diesel engine
Piston
Performance and emission

* Corresponding author:

T. Chandrashekar
E-mail: chandru.t222@gmail.com

Received: 4 June 2025
Revised: 14 July 2025
Accepted: 19 August 2025

A B S T R A C T

In this investigation, we examined how a thermal barrier-coated piston affects the performance and emission characteristics of a diesel engine operating on diesel fuel. We fully coated the piston crown's top surface with thermal barrier coating (TBC) materials $Sm_2Zr_2O_7$ as the top coat (300 µm thick) and Al_2O_3-13%TiO_2 as the bond coat (200 µm thick) using the plasma spray technique. We conducted experiments under varying load conditions using a four-stroke, single-cylinder diesel engine. Our results show that the coated engine achieved a 14% increase in brake thermal efficiency and up to a 27.03% reduction in brake specific fuel consumption compared to the uncoated engine. Additionally, the coated engine reduced carbon monoxide (CO) and hydrocarbon (HC) emissions by 50% and 66%, respectively, while carbon dioxide (CO_2) and nitrogen oxide (NOx) emissions increased by 33% and 293 ppm due to improved combustion efficiency and higher in-cylinder temperatures.

© 2025 Published by Faculty of Engineering

1. INTRODUCTION

In today's economically competitive world, there is a significant decline in crude oil fuel resources, which creates an urgent need for enhancing efficiency of internal combustion engines. In particular, compression ignition (CI) diesel engines are considerably more efficient at producing torque than other fuel engines because of their high compression ratio. Diesel engines play a crucial role in both the transportation and agricultural sectors due to their economic advantages, high torque output at low speeds (enabled by high compression ratios), and lower running costs. It also explains that in diesel engines, the chemical energy from fuel is transformed into mechanical work through combustion in the combustion chamber at high pressure and temperature. However, not all of this energy is converted into useful work because some of it is lost as heat through the cooling system, the combustion chamber walls, and other engine parts. Furthermore, the piston is a crucial component within the combustion chamber, where it absorbs a significant amount of heat energy generated during the combustion process.

This heat absorption can shorten the piston's lifespan. To address this issue, certain parts of combustion chamber in low heat rejection engines, also known as thermal barrier engines, are coated with heat-resistant materials to reduce heat loss and enhance efficiency.

Many investigators have investigated that engines coated with thermal barrier coating (TBC) enhance performance and reduce emissions. One investigator [1] reported that average heat flux of piston crowns coated with YPSZ and NiCrAl was 98% lower than that of piston crowns left uncoated. Another researcher [2] demonstrated that thermal insulation coatings in low heat rejection (LHR) engines can lead to lower fuel consumption and higher volumetric performance. A separate study [3] showed that thermal barrier coatings decrease cycle-averaged heat losses via the walls, and TBC and surface roughness significantly impact hydrocarbon emission reductions. Furthermore, an investigator [4] found that by partially combining ZrO_2 with 8YSZ and modifying physical and chemical structure of 8YSZ, these coating materials is capable of withstanding temperatures exceeding 1600°C while improving stress relaxation.The findings of multiple researchers emphasize the impact of TBC on engine pistons, particularly in enhancing thermal resistance and improving engine performance. It notes that TBC significantly increase surface temperature of the piston, creating a high-temperature combustion chamber that improves efficiency [5]. For instance, one study showed that applying YSZ coating to pistons improved brake thermal efficiency by 3–5%, reduced heat loss by 5–10%, and lowered brake-specific fuel consumption by up to 28.9%, while also cutting carbon monoxide emissions [6]. Other studies reported similar benefits, including increases in brake thermal and mechanical efficiency, fuel consumption reductions, and CO emissions [7]. Additional research found that TBC with low thermal conductivity raised the piston surface temperature by up to 48%, while functionally graded coatings improved the maximum surface temperature of Al–Si alloy and steel pistons by 28% and 17% respectively [8,9]. Finally, thermal barrier coatings containing TiO_2 also showed enhanced corrosion resistance [10]. A recyclable CNT–CuO nanocatalyst enabled 96 % Jatropha biodiesel yield, while hydrogen-enriched ammonium hydroxide emulsification enhanced engine performance and cut NOx, HC, and CO emissions for sustainable diesel applications [11]. Enriching a 30 % GHME–diesel blend with CuO, CNTs, or CuO–CNT nanocomposites improved diesel engine efficiency, reduced emissions, and lowered costs, with CNTs delivering the greatest performance gains, CuO cutting fuel cost by 5.42 %, and the CuO–CNT composite providing the most balanced benefits for sustainable operation [12]. ZnS nanoparticle-enhanced water-emulsified diesel with ESP integration achieves stable performance, reduces NOx, HC, CO, and PM emissions, offering an effective combined strategy for cleaner and more sustainable diesel combustion [13]. Using Box–Behnken optimization, this study identified 15.2 % MES, 14.9 % AH, and 5.2 % EGR as the optimal CNT-enriched diesel blend, achieving statistically validated improvements in performance and emissions for sustainable engine operation [14]. Using Box–Behnken optimization, this study identified a diesel blend containing maximum WLPO, 11.9 % HH, and 93.2 ppm Al_2O_3 nanocatalyst as optimal, delivering statistically validated gains in performance and emission reduction while reducing fossil fuel use by ~42 %, thereby advancing sustainable energy goals [15]. Al_2O_3 nanoparticle-enriched Bauhinia malabarica biodiesel–diesel blends, combined with electrostatic precipitators, enhanced brake thermal efficiency, lowered most emissions, and achieved a net 54.2 % particulate matter reduction, offering a cleaner and more efficient fuel strategy [16].

Literature findings indicate that engines coated with thermal barrier coatings generally demonstrate improved brake thermal efficiency and reduced brake-specific fuel consumption, which also contributes to lower CO_2 and hydrocarbon emissions. Investigators agree that thermal barrier coatings enhance the thermal efficiency of LHR engines, although brake-specific fuel consumption is sometimes slightly higher in these systems [17]. The experimental work mentioned in this study was performed on four-stroke diesel engines, single-cylinder, utilizing Sm-ZrO_2 and Al_2O_3–13%TiO_2 coatings applied to the piston crowns [18]. Despite extensive research on thermal barrier coatings,

limited studies have evaluated the combined thermal and tribological performance of Sm-ZrO_2 and Al_2O_3–13%TiO_2 coatings under realistic engine operating conditions [19]. This study aims to address that gap by experimentally evaluating the impact of these coatings on a single-cylinder, four-stroke diesel engine, focusing on improvements in thermal efficiency, and emissions. Table 1 presents the key properties of various TBC materials.

Table 1 Different TBC compositions and their mechanical and thermal behavior [20]

Materials	Thermal expansion 10–6 (1/ °C)	Thermal conductivity (w/m °C)	Poisson's ratio	Young's modulus (GPa)
$Sm_2Zr_2O_7$	10.1	2.1	0.27	220
AT13	16	67	0.31	110
Alsi	21	155	0.30	90
NiCrAl	12	16.1	0.27	90

2. MATERIALS AND METHODS

2.1 Coating material

In the AT13 coating, 87% Al_2O_3 primarily contributes to strong interfacial bonding, while the remaining 13% TiO_2 enhances corrosion resistance. Among various ceramic materials, $Sm_2Zr_2O_7$ is selected due to its notably low thermal conductivity. The piston crown and top surface of the engine was coated using the plasma spray technique. Prior to coating, 500 µm of material was removed from the piston surface through machining to maintain the original compression ratio of the LHR (Low Heat Rejection) engine, ensuring it remained consistent with the uncoated engine [21,22]. The volume of material removed was carefully matched to the volume of the thermal barrier coating (TBC) to be applied. After machining, the piston crown was grid-blasted to prepare the surface. It was then coated with a 200 µm layer of Al_2O_3–13%TiO_2 bond coat, which provides oxidation resistance and serves as a foundation for insulation. Following this, a 300 µm top coat of $Sm_2Zr_2O_7$ was applied using an atmospheric plasma spray gun [23]. The total coating thickness restored the piston to its original dimensions.

2.2 Sem analysis of the coating material

The scanning electron microscopy image of TBC applied to the piston is presented in Figure1, referencing studies [24,25]. This image helps visualize microstructure and quality of the coating on the piston surface. Fig.1 illustrates that TBC on piston comprises a bilayer structure [26]. The first layer, with a thickness of 200 µm, consists of AT13, a composite material containing 87% Al_2O_3 and 13% TiO_2. Second layer, applied over the first, is 300 µm thick and composed of $Sm_2Zr_2O_7$, comprising 92% ZrO_2 and 8% Sm_2O_3 [27]. The total thickness of the coating deposited on the piston surface is 500 µm.

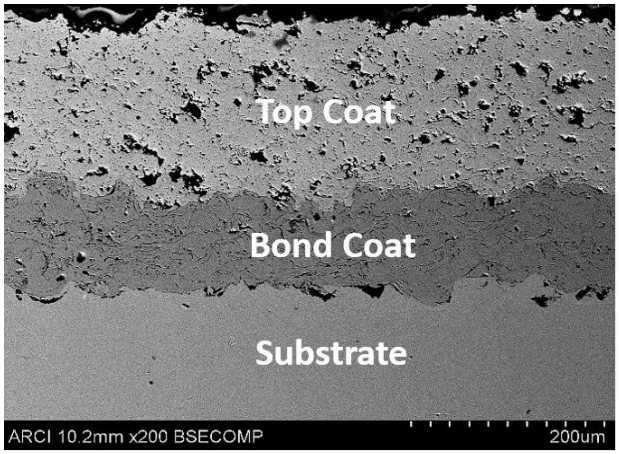

Fig. 1. Scanning image of TBC.

2.3 Plasma spray technique

Several coating techniques are available, including plasma arc deposition, chemical vapor deposition (CVD), thermal plasma spraying, and physical vapor deposition (PVD). In this investigation, the thermal plasma spray approach is implemented to apply the coating. Both coated and uncoated pistons are depicted in Figures 2 and 3, correspondingly [28,29]. An electric arc of high frequency is produced between a tungsten cathode and piston. A high-temperature plasma plume is directed towards substrate surface as gas passing through inter-electrode gap becomes ionised. Approximate plasma temperatures

range from 1,800°C to 14,500 °C. Coating powder is introduced near the gas nozzle, where it is rapidly melted by the plasma and propelled onto the piston surface to form the coating. The schematic of plasma spray process has been depicted in Figure 4 [30].

Fig. 2. Uncoated piston.

Fig. 3. TBC piston.

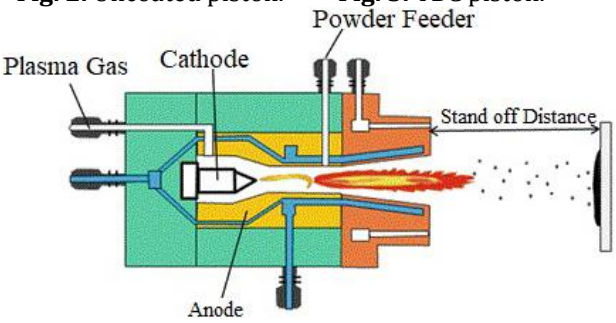

Fig. 4. Plasma-spray process

3. EXPERIMENTAL SETUP

The experimental setting comprises of a four-stroke CI engine with a variable compression ratio (VCR) that operates at a constant speed of 1500 rpm. Loading device is an eddy current dynamometer, which is further supported by a water cooling system and a lubrication system. Figures 5 and 6 illustrate the experimental setup's actual photograph and schematic diagram, correspondingly. Table 2 comprises test engine's specifications. The compression ratio of the VCR engine used in study ranges from 14 to 17.5. The VCR engine is tested under various loading conditions: 0 to 9 kg, with 9kg representing maximum load capacity of engine. The inlet and outlet temperatures of cooling water, exhaust gas outlet, and air intake manifold are monitored by a number of temperature sensors positioned in strategic locations. The in-cylinder combustion pressure is measured employing a piezoelectric (PIZO-type) sensor. The engine performance and parameters are monitored using Soft View engine analysis software. Exhaust emissions are evaluated using an exhaust gas analyzer, measuring concentrations of CO (%), O_2 (%), CO_2 (%), HC (ppm), and NO_x (ppm).

The experimental tests were carried out on a single-cylinder, four-stroke diesel engine using both uncoated and TBC-coated pistons. Each test was performed under six different load conditions (0, 1.5, 3, 4.5, 6, and 7.5 kg). For each load condition, the measurements were repeated three times to ensure repeatability and reduce random errors. The average values were taken for analysis. The engine with the uncoated piston was used as the control setup to compare the performance and emission characteristics against the TBC-coated engine.An emission test was also conducted using an AVL Five Gas Analyzer.

(a)

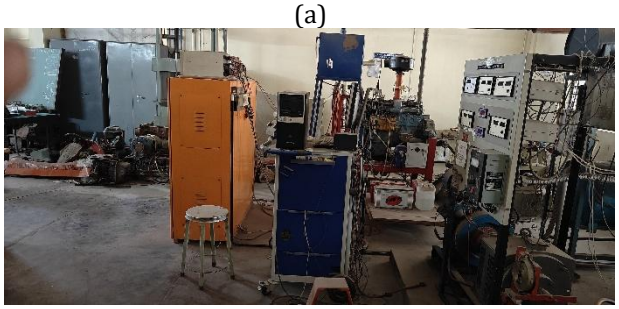

(b)

Fig.5. a, b Experimental setup (photographic view).

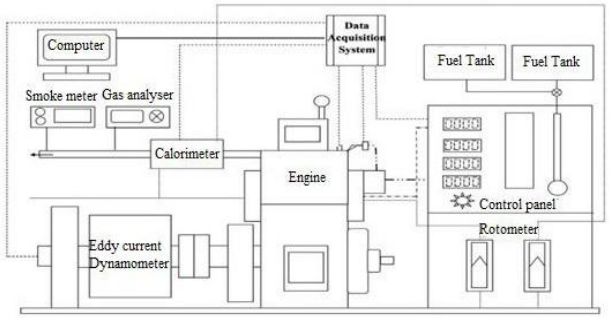

Fig. 6. Expermental setup (schematic view).

Table 2. Engine technical specification.

Parameters	Specifications
Engine	Single cylinder, air cooled, four-stroke diesel, rated power 7.4kW at 1500rpm, stroke 116mm, bore 102mm. 948CC, compression ratio 17.5.
Dynamometer	Eddy current is air-cooled, with a loading unit.
Exhaust gas analyzer	AVL Five gas analyzer
Rota meter	Engine cooling 40 to 400 LPH; calorimeter 25 to 250 LPH.

3.1 Error margins and uncertainty levels

Engine performance and emissions were carefully monitored throughout the experimental process. To ensure accuracy and reliability, regular calibration of the engine performance instruments and gas analyzers was conducted. Once the engine reached a steady-state operating condition, critical emission parameters such as carbon monoxide (CO), carbon dioxide (CO_2), hydrocarbons (HC), and nitrogen oxides (NO_x) were measured and recorded manually using calibrated emission analyzers.

Table 3. Error margins and uncertainty levels.

Measurement	Instrument	Accuracy	Uncertainty
Fuel consumption	Burette	±0.2 cc	1.5
Loading device	Load cell	±0.1kg	0.1
Speed	Speed sensor	±10 rpm	1
Exhuast gas measurement	Temperature indicator	±2 °C	0.30
CO	Exhaust gas analyzer	±0.02%	0.02
CO_2		±0.02%	0.02
HC		±10 ppm	0.1
NO_x		±12 ppm	0.2
Cylinder pressure	Pressure transducer	±0.3 kg	0.3
Crank angle	Crank angle encoder	±1°	1

The uncertainties associated with each measured parameter are systematically presented in Table 3. To quantify the total experimental uncertainty, Holman's methodology was employed. This method allows for a comprehensive evaluation by combining individual error sources in a statistically valid manner. Based on this analysis, the total percentage uncertainty across all measured and calculated parameters in this experiment was determined to be ±2.119%.

4. RESULT AND DISCUSSION

4.1 Comparison

Brake thermal efficiency (BTE) variation for engines coated with YSZ, YPSZ, and $Sm_2Zr_2O_7$ thermal barrier coatings is shown in Figure 7. YSZ had the lowest BTE of all the materials tested, at 24.0% [31], while YPSZ improved to 30.4% [32], suggesting better thermal insulation and fewer heat losses. Since the $Sm_2Zr_2O_7$-coated engine has a lower thermal conductivity and better phase stability at higher temperatures, it retains heat better in the combustion chamber and converts fuel energy into useful work more effectively. This is why it achieved the highest BTE of 32.3%. The trend shows that engine efficiency can be greatly increased by using sophisticated ceramic coatings with ideal thermal characteristics.

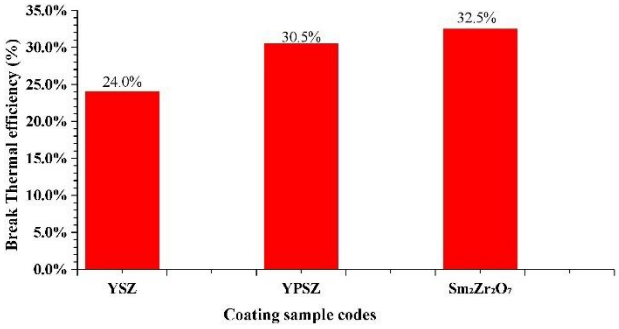

Fig. 7. Comparison with other TBC coating materials.

4.2 Heat balance of engine

Table 4 presents the heat balance sheet for both the uncoated engine and the engine with a thermal barrier coating operating at maximum load. Figure 8 compares the heat distribution and the percentages of total heat generated during combustion that are distributed as useful heat, heat loss to coolant, exhaust heat loss, and unaccounted losses.

Table 4. Heat balance sheet.

Heat distribution	Uncoated engine at 9 kg load (%)	Coated engine at 9 kg load (%)
Heat utilized	28.5	32.5
Heat lost	37.6	35.40
Heat exhaust	12.2	15.96
Heat unaccounted	21.6	16.50

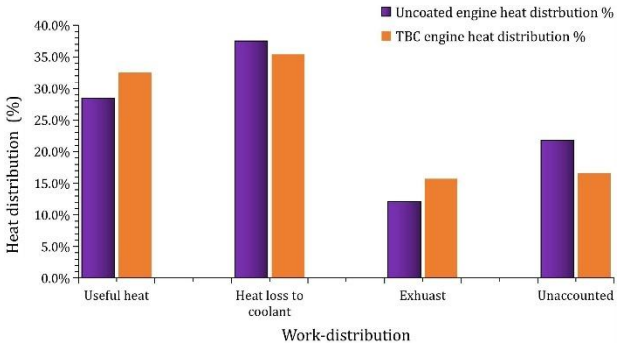

Fig. 8. Heat balance sheet for 9 kg load.

The TBC engine shows a higher proportion of useful heat compared to the uncoated engine, indicating improved thermal efficiency due to reduced heat transfer to the cooling system. Heat loss to the coolant is slightly lower for the TBC engine, confirming the insulating effect of the coating. However, exhaust heat losses are marginally higher in the TBC engine, likely because more heat is retained in the combustion gases rather than dissipated through the engine walls. Unaccounted losses are slightly reduced for the TBC engine, suggesting better overall heat utilization.

This trend confirms that thermal barrier coatings effectively minimize heat rejection to the coolant, enabling more energy to be converted into useful work.

4.3 Heat release rate (HRR)

Figure 9 shows the heat release rate (HRR) for TBC-coated and uncoated engines at maximum load. The TBC engine exhibits a higher peak HRR of 61.85 J/°deg compared to 43.0 J/°deg for the uncoated engine. The peak occurs at 5° after Top dead center (TDC),with the increase starting around 3° before TDC. The HRR is higher in coated engines because the thermal barrier on the piston crown keeps more heat inside the combustion chamber. This helps the fuel burn more completely and quickly, leading to more heat being released during combustion [33].

Figure 10 compares in-cylinder pressure versus crank angle at full load for TBC-coated and uncoated engines. Combustion starts earlier in the TBC engine (13° BTDC) than in the uncoated one (11° BTDC), indicating reduced ignition delay. The TBC engine also shows a higher peak pressure of 59.33 bar, which is 12.23% greater than the uncoated engine (51.92 bar). Because more fuel burns during the premixed stage of TBC-coated engines, which produces more heat, LHR engines exhibit higher peak pressure in the combustion chamber [34].

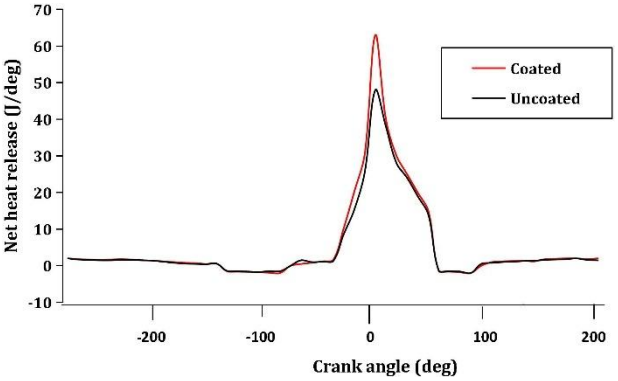

Fig. 9. Heat release rate of uncoated & TBC engine.

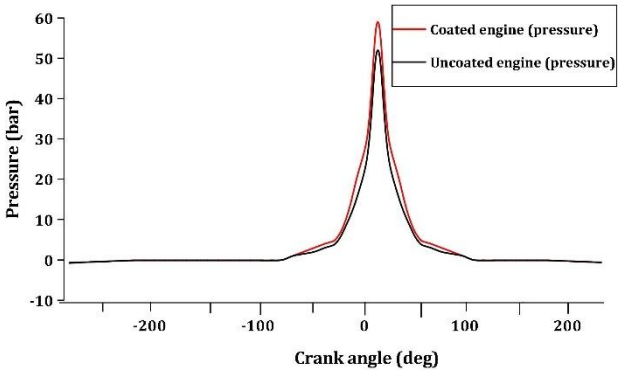

Fig. 10. Pressure changes Uncoated and TBC coated.

4.4 Brake thermal efficiency

Figure 11 illustrates the difference in brake thermal efficiency (BTE) between the uncoated (UC) and thermal barrier coated (TBC) engines under all load conditions. The TBC-coated engine consistently exhibits higher efficiency than the uncoated engine across all load" levels, as evidenced by figure. The TBC-coated piston achieves a brake power of 32.5% at maximal load of 9 kg, compared to 28.5% with uncoated piston. This represents a peak improvement of 14% in BTE. This may be due to the addition of co-doping to the $Sm_2Zr_2O_7$, which can reduce the overall thermal conductivity of the TBC material and enhance its sintering resistance at high temperatures. The lower thermal conductivity of the TBC material increases thermal resistance on the piston surface, which in turn reduces heat transfer. This retained heat contributes to improved thermal efficiency [35].

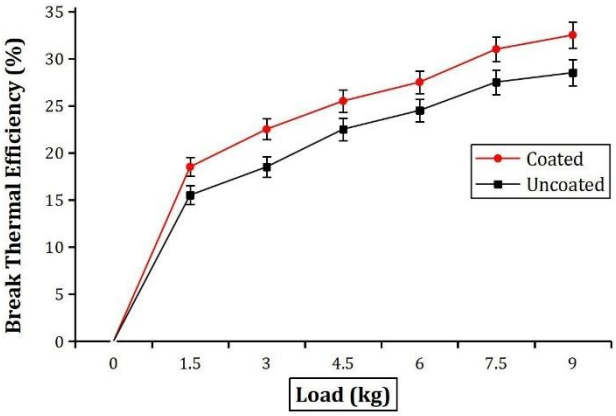

Fig. 11. Brake thermal efficiency of uncoated and TBC coated engine.

4.5 Volumetric efficiency

The thermal coating maintains elevated temperatures within the LHR engine cylinder, promoting more complete combustion of the air–fuel mixture. This increases the temperature and density of the residual gases, which lowers the density of the inducted air. The high cylinder temperature in the LHR engine reduces the volumetric efficiency. Volumetric efficiency of the TBC-coated engine was measured at 79.29%, compared to 80.60% for the uncoated engine. This represents a reduction of 1.31% in volumetric efficiency when engine operated at load of 9kg. Across all load conditions, the TBC-coated engine consistently demonstrated lower volumetric efficiency than uncoated engine. Volumetric efficiency refers to amount of fresh air drawn into engine during suction stroke. Figure 12 illustrates differences in volumetric efficiency between the uncoated and TBC-coated engines under various load conditions, clearly showing that TBC-coated engine achieves low efficiency at every load [36].

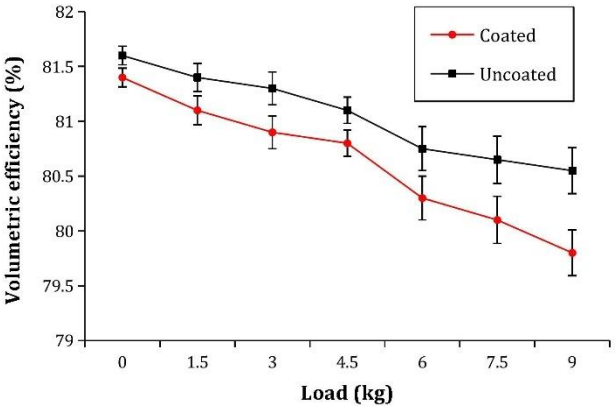

Fig. 12. Volumetric efficiency of Uncoated and TBC coated engine

4.6 Brake-specific fuel consumption (BSFC)

Figure 13 presents the brake-specific fuel consumption (BSFC) of both the TBC-coated engine and the uncoated (UC) engine under various load conditions. Findings highlighted that TBC-coated engine consistently exhibits lower BSFC than standard uncoated engine. Specifically, at a load of 9 kg, the BSFC for uncoated engine is 0.37 kg/kWh, while for the TBC-coated engine it is reduced to 0.27 kg/kWh—a decrease of 27.03%.

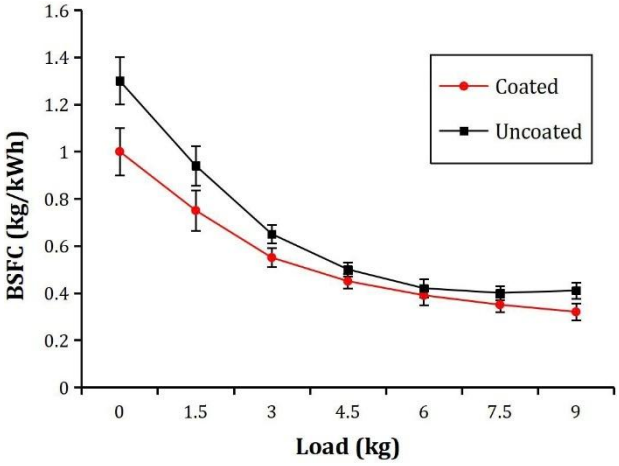

Fig. 13. Brake-specific fuel consumption of uncoated and TBC coated engine.

Typically, engines require more fuel to maintain constant rpm under load. However, thermal barrier coating enhances combustion efficiency by retaining more heat within the combustion chamber. This improved thermal retention allows the TBC-coated engine to maintain rpm without additional fuel, thereby reducing unburned fuel wastage and lowering BSFC. The overall reduction in brake-specific fuel consumption can be attributed to better energy conservation and higher combustion chamber temperatures in the TBC-coated engine across all load conditions.

4.7 Carbon monoxide (CO)

Carbon monoxide (CO) emissions are primarily produced when combustion is incomplete, often due to lower temperatures in the combustion chamber. Figure 14 displays the measured CO emission for the TBC-coated engine is 0.01%, compared to 0.02% for the uncoated engine representing a 50% reduction.

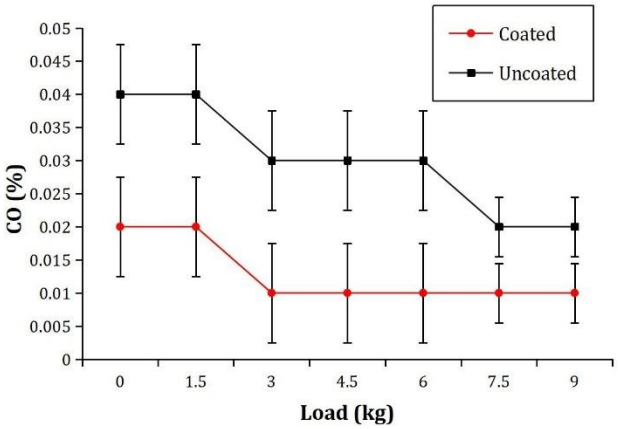

Fig. 14. Carbon monoxide of Uncoated and TBC coated engine.

In uncoated engine Low combustion temperatures or oxygen-deficient conditions prevent full oxidation of carbon to CO_2, thus increasing CO emissions.

$$C_xH_y+O_2 \rightarrow CO+H_2O \quad (1)$$

In a TBC-coated engine, higher in-cylinder temperatures enhance oxidation, converting more CO into CO_2, thereby reducing CO emissions.

$$C_xH_y+O_2 \rightarrow CO_2+H_2O \quad (2)$$

In contrast, the TBC-coated engine, which maintains higher combustion chamber temperatures, achieves more complete combustion and thus emits less CO. This decrease in CO emissions is attributed to improved combustion efficiency in TBC-coated engine.

4.8 Carbon dioxide (CO_2)

Figure 15 illustrates the CO_2 emission levels of both the TBC-coated engine and uncoated (UC) engine under various load conditions. Results show that TBC-coated engine produces higher CO_2 emissions than the uncoated engine, primarily due to more complete combustion. This complete combustion allows the TBC engine to convert more fuel into useful energy, resulting in a slight increase in CO_2 output. Experimentally, at a load of 9kg and an engine speed of 1500rpm, the CO_2 emission for the TBC-coated engine is 1.2%, while for the uncoated engine it is 0.9%, representing a 33.33% increase. This increase in CO_2 emissions is a direct result of improved combustion efficiency in the TBC-coated engine.

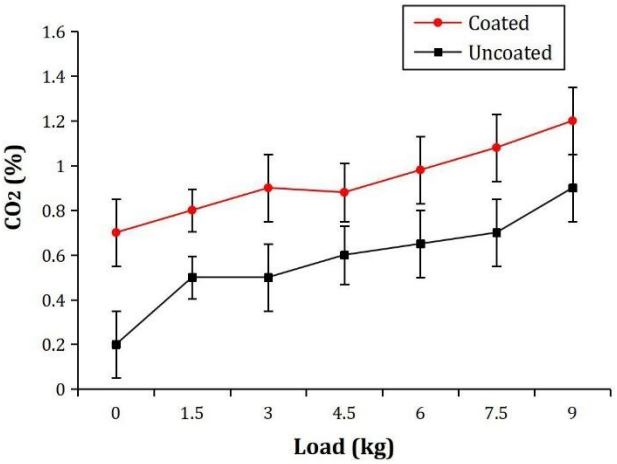

Fig. 15. Carbon dioxide of Uncoated and TBC coated engine.

4.9 Hydrocarbons (HC)

Figure 16 presents the hydrocarbon (HC) emissions of both TBC-coated engine and the uncoated (UC) engine under various load conditions. In uncoated engine, HC is high due to fuel escaping the combustion chamber before complete oxidation and quenching of the flame near cylinder walls.

$$C_xH_y \rightarrow \text{Unburned HCs} \quad (3)$$

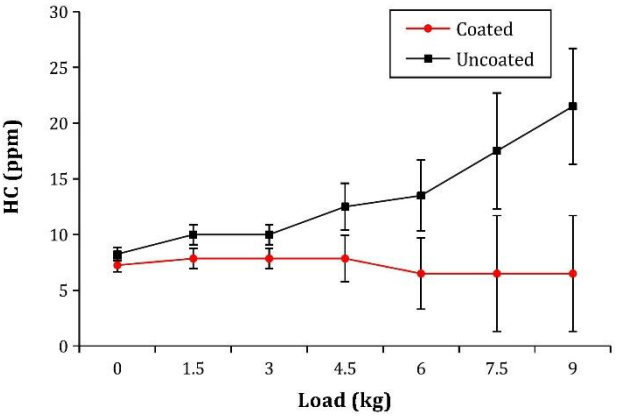

Fig. 16. Hydrocarbons of Uncoated and TBC coated engine.

TBC engine reduces wall heat losses, increasing surface temperatures and minimizing flame quenching. This leads to more complete combustion and lower HC emissions. HC emission for the TBC-coated engine is 7ppm, compared to 21 ppm for the uncoated engine—a reduction of 66.67%. Overall, the TBC-coated engine consistently exhibits much lower HC emissions than the uncoated engine at all load levels.

4.10 Nitrogen oxides (NO_x)

Figure 17 displays the nitrogen oxide (NOx) emissions for uncoated (UC) engines and TBC-coated engines under various load conditions. Results indicate that NOx emissions are higher in TBC-coated engine. Increases in-cylinder temperature, especially during peak combustion. Enhances combustion efficiency, leading to more complete fuel burning. However, NO_x formation follows the Zeldovich mechanism, which is highly temperature-dependent

$$N_2+O \rightarrow NO+N \quad (4)$$

$$N+O_2 \rightarrow NO+O \quad (5)$$

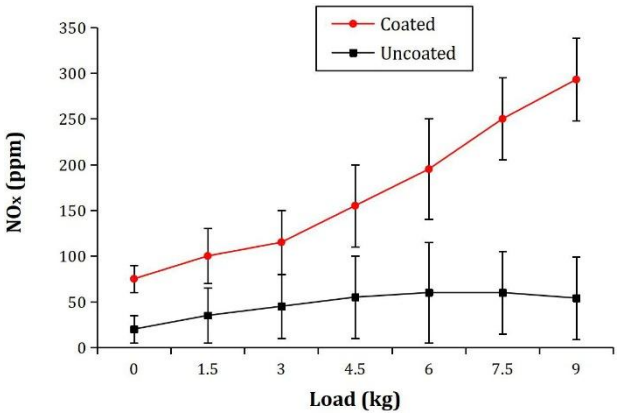

Fig. 17. Nitrogen oxides of uncoated and TBC coated engine.

These reactions become more active at temperatures above ~1800 K. Since TBCs raise the combustion temperature beyond this threshold, NO_x generation intensifies. This finding is consistent with previous research [37,38] has shown that low heat rejection (LHR) engines, such as those with thermal barrier coatings, tend to produce higher NOx levels. Increase in NOx (293 ppm) emissions can be attributed to higher combustion chamber temperatures, a longer combustion duration, and a greater proportion of fuel being burned.

To counterbalance this drawback and meet emission standards, Exhaust Gas Recirculation (EGR) are commonly adopted. It works by recirculating a portion of exhaust gas back into the intake, which lowers the oxygen level and peak combustion temperature key factors in NO_x formation via the Zeldovich mechanism. EGR helps suppress NO_x by keeping the flame temperature in check. However, using too much EGR can reduce combustion efficiency, leading to higher CO and HC emissions. So, an optimal EGR rate is essential for balancing performance and emissions.

5. CONCLUSION

The conversion of a computerized compression ignition (CI) single-cylinder diesel engine to a Low Heat Rejection (LHR) engine involves coating the piston surface with a 500 µm layer of $Sm_2Zr_2O_7$ (Samarium zirconate) as the top coat and AT13 (a bond coat material) using thermal plasma spray techniques. The conclusions derived from the experimental work are outlined below.

- The TBC-coated engine delivers a 31% higher peak heat release rate (HRR) and generates 12.23% greater peak cylinder pressure than the uncoated engine.
- At maximum load, it achieves a peak brake thermal efficiency of 14%, significantly outperforming the uncoated engine. It also reduces brake specific fuel consumption by 27.03%.
- In terms of emissions, the TBC-coated engine cuts carbon monoxide and hydrocarbon emissions by 50% and 66%, respectively.
- However, due to more complete combustion and higher in-cylinder temperatures, it raises carbon dioxide emissions by 33% and increases nitrogen oxide levels, peaking at 293 ppm, compared to the uncoated engine.

Future research should evaluate the durability of TBC coatings under long-term and cyclic engine conditions. Testing on multi-cylinder engines is recommended to confirm scalability. To address higher NO_x emissions, future work could also explore EGR or after-treatment systems alongside TBC applications.

Acknowledgement

I am very grateful to the management and HOD Department of Mechanical engineering, Dr. Ambedkar Institute of Technology, Bengaluru for letting me do my research work there.

REFERENCES

[1] H. A. Jalaludin, S. Abdullah, M. J. Ghazali, B. Abdullah, and N. R. Abdullah, "Experimental Study of Ceramic Coated Piston Crown for Compressed Natural Gas Direct Injection Engines," *Procedia Eng.*, vol. 68, pp. 505–511, Jan. 2013, doi: 10.1016/j.proeng.2013.12.213.

[2] A. Poubeau, A. Vauvy, F. Duffour, J.-M. Zaccardi, G. d. Paola, and M. Abramczuk, "Modeling investigation of thermal insulation approaches for low heat rejection Diesel engines using a conjugate heat transfer model," *Int. J. Engine Res.*, vol. 20, no. 1, pp. 92–104, Dec. 2018, doi: 10.1177/1468087418818264.

[3] J. Somhorst, M. Oevermann, M. Bovo, and I. Denbratt, "Evaluation of thermal barrier coatings and surface roughness in a single-cylinder light-duty diesel engine," *International Journal of Engine Research*, vol. 22, no. 3, pp. 890–910, Oct. 2019, doi: 10.1177/1468087419875837

[4] K. Dychtoń, M. Drajewicz, M. Pytel, P. Rokicki, and A. Nowotnik, "Yttria-stabilized zirconia–alumina composite sintering temperature effect on thermal diffusivity," *J. Thermal Anal. Calorimetry*, vol. 126, no. 1, pp. 1–7, Aug. 2016, doi: 10.1007/s10973-016-5788-9M.

[5] M. Cerit and M. Coban, "Temperature and thermal stress analyses of a ceramic-coated aluminum alloy piston used in a diesel engine," *International Journal of Thermal Sciences*, vol. 77, pp. 11–18, Mar. 2014, doi: 10.1016/j.ijthermalsci.2013.10.009.

[6] G. Sivakumar and S. Senthil Kumar, "Investigation on effect of Yttria Stabilized Zirconia coated piston crown on performance and emission characteristics of a diesel engine," *Alexandria Eng. J.*, vol. 53, no. 4, pp. 787–794, Dec. 2014, doi: 10.1016/j.aej.2014.08.003.

[7] A. Vadivel and S. Periyasamy, "Experimental Investigation of Thermal Barrier (8YSZ-MGO-TIO2) Coated Piston used in Diesel Engine," *Journal of Applied Fluid Mechanics*, vol. 13, no. 4, pp. 1157–1165, Mar. 2020, doi: 10.36884/jafm.13.04.30825.

[8] E. Buyukkaya and M. Cerit, "Thermal analysis of a ceramic coating diesel engine piston using 3-D finite element method," *Surf. Coatings Technol.*, vol. 202, no. 2, pp. 398–402, Nov. 2007, doi: 10.1016/j.surfcoat.2007.06.006.

[9] E. Buyukkaya, "Thermal analysis of functionally graded coating AlSi alloy and steel pistons," *Surf. Coatings Technol.*, vol. 202, no. 16, pp. 3856–3865, May 2008, doi: 10.1016/j.surfcoat.2008.01.034.

[10] S.-K. Jia, Y. Zou, J.-Y. Xu, J. Wang, and L. Yu, "Effect of TiO2 content on properties of Al2O3 thermal barrier coatings by plasma spraying," *Transactions of Nonferrous Metals Society of China*, vol. 25, no. 1, pp. 175–183, Jan. 2015, doi: 10.1016/s1003-6326(15)63593-2.

[11] S. Vellaiyan, "Improved jatropha biodiesel yield and engine performance using carbon nanotube-copper oxide nanocatalyst and ammonium hydroxide emulsion for scalable clean energy solutions," *Biomass and Bioenergy*, vol. 201, p. 108120, Jun. 2025, doi: 10.1016/j.biombioe.2025.108120.

[12] S. Vellaiyan, "Comparative evaluation of nanoparticle-enriched Gossypium hirsutum methyl ester blends for enhanced energy, emission, and economic performance in diesel engines," *Cleaner Eng. Technol.*, vol. 27, p. 101004, Jul. 2025, doi: 10.1016/j.clet.2025.101004.

[13] B. S. Aljohani, K. Aljohani, M. Kandasamy, S. Vellaiyan, and B. Nagappan, "Enhancement of Diesel Engine Performance and Emission Reduction Using ZnS Nanoparticles and Water Emulsions with Electrostatic Precipitator Integration," *Case Studies in Thermal Engineering*, p. 106157, Apr. 2025, doi: 10.1016/j.csite.2025.106157.

[14] S. Vellaiyan, "Optimization of Spirulina biodiesel-ammonium hydroxide blends with exhaust gas recirculation for enhanced diesel engine performance and emission reduction," *Results Eng.*, vol. 26, p. 105015, Jun. 2025, doi: 10.1016/j.rineng.2025.105015.

[15] S. Vellaiyan, "Development of sustainable diesel fuel blend using biodiesel, hydrous hydrazine and nanocatalysts for optimized performance and emission control," *Case Stud. Thermal Eng.*, vol. 69, p. 105966, May 2025, doi: 10.1016/j.csite.2025.105966.

[16] S. Vellaiyan, "Enhancement of Combustion Performance and Emission Control in Bauhinia Malabarica Biodiesel-Diesel Blends Using Aluminium Oxide Nanoparticles and Electrostatic Precipitators," *Cleaner Eng. Technol.*, p. 100981, Apr. 2025, doi: 10.1016/j.clet.2025.100981.

[17] T. Powell *et al.*, "Experimental investigation of the relationship between thermal barrier coating structured porosity and homogeneous charge compression ignition engine combustion," *Int. J. Engine Res.*, vol. 22, no. 1, pp. 88–108, Jul. 2019, doi: 10.1177/1468087419843752.

[18] J. Balaji, M. M. Nataraja, K. Sadashiva, and S. Supreeth, "Experimental and Computational Analysis of Thermal Characteristics of Polymer Resin Reinforced with Rice Husk and Aluminium Nitride Filler Composites," *Journal of The Institution of Engineers (India): Series D*, vol. 105, pp. 313-321, Apr. 2023, doi: 10.1007/s40033-023-00480-z.

[19] A. M. Doddamani, I. G.Bhavi, R. Noorahmed, M. B. Vanarotti, J. Balaji, and S. Sameer Hussain, "Studies on Physical, Mechanical & Tribological Properties of Al6063 Incorporated with CNT & Nano Clay as Filler Materials," *Tribol. Industry*, vol. 46, no. 4, pp. 722–735, Dec. 2024, doi: 10.24874/ti.1748.09.24.11.

[20] S. P. Jena, S. K. Acharya, H. C. Das, P. P. Patnaik, and S. Bajpai, "Investigation of the effect of FeCl 3 on combustion and emission of diesel engine with thermal barrier coating," *Sustain. Environ. Res.*, vol. 28, no. 2, pp. 72–78, Mar. 2018, doi: 10.1016/j.serj.2017.10.002.

[21] L. Gao, H. Guo, L. Wei, C. Li, and H. Xu, "Microstructure, thermal conductivity and thermal cycling behavior of thermal barrier coatings prepared by plasma spray physical vapor deposition," *Surf. Coatings Technol.*, vol. 276, pp. 424–430, Aug. 2015, doi: 10.1016/j.surfcoat.2015.06.033..

[22] H. M. Mobarak et al., "Effect of DLC Coating on Tribological Behavior of Cylinder Liner-piston Ring Material Combination When Lubricated with Jatropha Oil," *Procedia Eng.*, vol. 90, pp. 733–739, 2014, doi: 10.1016/j.proeng.2014.11.805.

[23] S. S. Pande, R. G. Tikotkar, J. Balaji, and S. Sameer Hussain, "Synergistic Reinforcing Influence of SiC, Al2O3, and CdS on Advanced Tribomechanical Properties of Aluminum Composites," *Tribol. Industry*, vol. 47, no. 7, pp. 64–76, Mar. 2025, doi: 10.24874/ti.1737.08.24.12.

[24] R. Gehlot and B. Tripathi, "Thermal analysis of holes created on ceramic coating for diesel engine piston," *Case Stud. Thermal Eng.*, vol. 8, pp. 291–299, Sep. 2016, doi: 10.1016/j.csite.2016.08.008.

[25] J. Balaji, M. M. Nataraja, and A. Rajesh, "Experimental investigation on mechanical properties of polymer composites reinforced with aluminium nitride & rice husk," *Mater. Today: Proc.*, vol. 52, pp. 1781–1787, 2022, doi: 10.1016/j.matpr.2021.11.445.

[26] E. Gingrich *et al.*, "The impact of piston thermal barrier coating roughness on high-load diesel operation," *International Journal of Engine Research*, vol. 22, no. 4, pp. 1239–1254, Dec. 2019, doi: 10.1177/1468087419893487.

[27] P. Pędrak, M. Drajewicz, K. Dychtoń, and A. Nowotnik, "Microstructure and thermal characteristics of SiC–Al2O3–Ni composite for high-temperature application," *J. Thermal Anal. Calorimetry*, vol. 125, no. 3, pp. 1353–1356, Jul. 2016, doi: 10.1007/s10973-016-5608-2.

[28] J. Wu, H. Guo, M. Abbas, and S. Gong, "Evaluation of plasma sprayed YSZ thermal barrier coatings with the CMAS deposits infiltration using impedance spectroscopy," *Prog. Natural Sci.: Mater. Int.*, vol. 22, no. 1, pp. 40–47, Feb. 2012, doi: 10.1016/j.pnsc.2011.12.007.

[29] V. Garud *et al.*, "Performance and CombustionCharacteristics of Thermal Barrier coated (YSZ) Low heat rejection diesel engine," *Materials Today Proceedings*, vol. 4, no. 2, pp. 188–194, Jan. 2017, doi: 10.1016/j.matpr.2017.01.012.

[30] D. Das, G. Majumdar, R. S. Sen, and B. B. Ghosh, "The Effects of Thermal Barrier Coatings on Diesel Engine Performance and Emission," *J. Institution Engineers (India): Ser. C*, vol. 95, no. 1, pp. 63–68, Jan. 2014, doi: 10.1007/s40032-014-0104-6.

[31] T. Karthikeya Sharma, "Performance and emission characteristics of the thermal barrier coated SI engine by adding argon inert gas to intake mixture," *J. Adv. Res.*, vol. 6, no. 6, pp. 819–826, Nov. 2015, doi: 10.1016/j.jare.2014.06.005.

[32] K. R. Sharma and G. Kumar, "Thermo-mechanical Experiments of Y-PSZ Thermal Barrier Ceramic Coating with Bond Coat of Alumina," *J. Institution Engineers (India): Ser. C*, vol. 96, no. 3, pp. 287–298, Jan. 2015, doi: 10.1007/s40032-015-0172-2.

[33] M. Prabhahar and K. Rajan, "Performance and combustion characteristics of a diesel engine with titanium oxide coated piston using Pongamia methyl ester," *J. Mech. Sci. Technol.*, vol. 27, no. 5, pp. 1519–1526, May 2013, doi: 10.1007/s12206-013-0332-3.

[34] B. Rajendra Prasath, P. Tamilporai, and M. F. Shabir, "Analysis of combustion, performance and emission characteristics of low heat rejection engine using biodiesel," *Int. J. Thermal Sci.*, vol. 49, no. 12, pp. 2483–2490, Dec, 2010, doi: 10.1016/j.ijthermalsci.2010.07.010.

[35] J. R. Nicholls, K. J. Lawson, A. Johnstone, and D. S. Rickerby, "Methods to reduce the thermal conductivity of EB-PVD TBCs," *Surf. Coatings Technol.*, vol. 151-152, pp. 383–391, Mar. 2002, doi: 10.1016/s0257-8972(01)01651-6.

[36] G. V. Reddy, N. G. Rasu, and T. H. Prasad, "Analysis of performance and emission characteristics of TBC coated low heat rejection engine," *International Journal of Ambient Energy*, vol. 42, no. 7, pp. 808–815, Jan. 2019, doi: 10.1080/01430750.2019.1567581.

[37] A. Şanlı, İ. T. Yılmaz, and M. Gümüş, "Investigation of combustion and emission characteristics in a TBC diesel engine fuelled with CH4–CO2–H2 mixtures," *Int. J. Hydrogen Energy*, vol. 46, no. 47, pp. 24395–24409, Jul. 2021, doi: 10.1016/j.ijhydene.2021.05.014.

[38] S. M. Abbas and A. Elayaperumal, "Experimental investigation on the effect of ceramic coating on engine performance and emission characteristics for cleaner production," *J. Cleaner Prod.*, vol. 214, pp. 506–513, Mar. 2019. doi: 10.1016/j.jclepro.2018.12.040.